UNIVERSITY OF BIRMINGHAM

On the use of ensemble predictions for parametric typhoon insurance

Ng, Kelvin; Leckebusch, Gregor; Ye, Qian; Ying, Wenwen; Zhao, Haoran

[Link to publication on Research at Birmingham portal](#)

On the Use of Ensemble Predictions for Parametric Typhoon Insurance

Kelvin S. Ng [1,*], Gregor C. Leckebusch [1,2] , Qian Ye [3], Wenwen Ying [4] and Haoran Zhao [4]

[1] School of Geography, Earth and Environmental Sciences, University of Birmingham, Birmingham B15 2TT, UK; g.c.leckebusch@bham.ac.uk
[2] Institute for Meteorology, Freie Universität Berlin, 12165 Berlin, Germany
[3] State Key Laboratory of Earth Surface Processes and Resource Ecology, Beijing Normal University, Beijing 100875, China; qianye@bnu.edu.cn
[4] Swiss Reinsurance Company Ltd., Beijing Branch, Beijing 100026, China; wenwen_ying@swissre.com (W.Y.); haoran_zhao@swissre.com (H.Z.)
[*] Correspondence: k.s.ng@bham.ac.uk

Abstract: Parametric typhoon insurances are an increasingly used financial tool to mitigate the enormous impact of tropical cyclones, as they can quickly distribute much-needed resources, e.g., for post-disaster recovery. In order to optimise the reliability and efficiency of parametric insurance, it is essential to have well-defined trigger points for any post-disaster payout. This requires a robust localised hazard assessment for a given region. However, due to the rarity of severe, landfalling tropical cyclones, it is difficult to obtain a robust hazard assessment based on historical observations. A recent approach makes use of unrealised, high impact tropical cyclones from state-of-the-art ensemble prediction systems to build a physically consistent event set, which would be equivalent to about 10,000 years of observations. In this study, we demonstrate that (1) alternative trigger points of parametric typhoon insurance can be constructed from a local perspective and the added value of such trigger points can be analysed by comparing with an experimental set-up informed by current practice; (2) the estimation of the occurrence of tropical cyclone-related losses on the provincial level can be improved. We further discuss the potential future development of a general tropical cyclone compound parametric insurance.

Keywords: tropical cyclone; disaster risk reduction; parametric insurance; extreme events; typhoons

1. Introduction

Tropical cyclones (TCs) have tremendous socioeconomic impact on East Asia, and especially China. On average, six to seven TCs with a tropical storm intensity of at least ($\geq$17.2 m/s) [1] make landfall in China every year [2]. For the 2018 typhoon season, the China Meteorological Administration (CMA) reported TC-related direct economic losses of over 67 billion RMB, and approximately 32 million people were affected [3]. Under the Sendai Framework for Disaster Risk Reduction 2015–2030 [4], cost-effective public and private investment in disaster risk reduction (DRR) for resilience is one of the priorities to reduce the impact of disasters. Financial instruments for risk transfer, such as (re)insurance solutions, are an important part of DRR due to their high benefit-cost ratio [5]. In particular, parametric insurance (or index-based insurance) would be suitable for respective DRR application. Unlike traditional insurance solutions, the payment of a parametric insurance does not depend on any post-event physical damage assessment. Once the agreed threshold(s), also known as trigger point(s), are exceeded, the compensation from the insurer would be made to the insuree. Given its low administrative costs and quick disbursement, parametric insurance can serve as a suitable financial instrument for DRR as it could speed up the post-disaster recovery significantly.

A first pilot programme of catastrophe parametric insurance in China was implemented in 2016 for ten cities in Guangdong [6]. The coverage increased to more cities

in subsequent years [6]. Currently, eighteen cities have such a parametric insurance arrangement [7]. The city governments who are involved in the programme first publish an invitation to tender, then primary insurers who are interested in offering such service would place a bid to compete for the contract. Primary insurers who have won such contracts include China Pacific Insurance (Group) Co., Ltd. (CPIC), People's Insurance Company of China Limited (PICC), and Ping An Insurance (Group) Company of China, Ltd. (PingAn) [8]. Swiss Reinsurance Company Ltd. (Swiss Re) has participated in this programme as a reinsurer since 2016. There are two major components in the catastrophe parametric insurance for respective cities in the Guangdong province: (1) parametric typhoon insurance, and (2) heavy rainfall parametric insurance [6,9]. The parametric typhoon insurance is triggered if the centre of the typhoon is located within a specific region, e.g., within 106 km radius from the city, and the intensity of typhoon, as reported by CMA, is above the agreed threshold value, e.g., 32.7 m/s [9]. The amount of compensation depends on the location and intensity of the typhoon. For example, in the period June 2021 to May 2022, the agreed compensation of parametric typhoon insurance for Zhuhai is 2 million RMB, if a typhoon is located within 106 km radius from the city with intensity, as estimated by CMA using the Dvorak technique [10] as 2-min mean maximum sustained wind [11], in the range of 32.7–36.9 m/s. The agreed compensation increases to 230 million RMB if the typhoon is located within a 46 km radius from the city with an intensity of at least 56.1 m/s [9]. In Guangdong, the twelve cities that are currently covered by the parametric typhoon insurance, are Jieyang, Shantou, Yangjiang, Chaozhou, Zhuhai, Huizhou, Shanwei, Maoming, Guangzhou, Dongguan, Jiangmen, and Zhanjiang [12–23]. Heavy rainfall parametric insurance, on the other hand, is triggered based on a complex index, which depends on multiple factors, including the intensity of heavy rainfall, and the extent of heavy rainfall. Currently, parametric typhoon insurance and heavy rainfall parametric insurance operate independently of each other. This means that in the case of a typhoon event, it is possible that both parametric insurances could be triggered or only one of the parametric insurances could be triggered. This study focuses on trigger points of parametric typhoon insurance only, as the main driver of the related hazards and wind speed is a classical variable to quantify the overall severity of an event. According to the World Meteorological Organization (WMO), TC is a generic term for a non-frontal synoptic scale cyclone which formed over tropical or sub-tropical oceans with organised convection and cyclonic surface wind [1]. Typhoon, on the other hand, is a special class of TC with intensity of 32.7 m/s or more [1]. Consequently, parametric typhoon insurance covers damages from typhoons, but not from all TCs.

The key to a suitable parametric insurance for DRR is to have a robust, optimal trigger point, i.e., realistic criteria that would be satisfied if disaster were to occur and the appropriate amount of compensation would be given to the insuree. If the trigger point is suboptimal, it could lead to over- or under-compensation. In the short term, the progress of post-disaster recovery could be delayed due to misallocation of resources. Consequently, in the long term, it will hinder the usefulness of this instrument for both agreeing parties. In practice, there are two major challenges in the development of the trigger point of a parametric typhoon insurance product:

(1)   Lack of consideration of the localised impact of typhoons; and
(2)   Lack of historical loss events for accurate loss occurrence estimation.

A typical approach, which attempts to address these issues, is to first construct an event set using a stochastic method based on historical observations to increase the potential sample size to compensate for the lack of historic events. The impact of stochastic TC events is then derived using simple models of TC structure [24–30]. While the stochastic approach is computationally inexpensive, the stochastic event set could be biased toward the past events and physically inconsistent, as discussed in Ng and Leckebusch (2021) [31].

In the context of the collaboration project INPAIS (Integrated Threshold Development for Parametric Insurance Solutions, https://www.birmingham.ac.uk/research/activity/environmental-health/projects/inpais.aspx (accessed on 11 October 2021)), a new approach,

the Osinski–Thompson approach [32,33] (sometimes referred to as the UNSEEN approach), is used to construct a high-impact TC event set. The underlying principle of the Osinski–Thompson approach is to aggregate all unrealised extreme events, which are generated from state-of-the-art ensemble prediction systems (EPSs), such that a large observational data set of extreme events can be constructed. These extreme events can be treated as real events as they are produced by the full physical models and cannot be distinguished a priori from later realised events. Various studies have employed the Osinski–Thompson approach to construct a climatologically consistent extreme windstorm event set to investigate European windstorms, Atlantic hurricanes, and Western North Pacific (WNP) typhoons [31,34,35].

Furthermore, Osinski et al. (2016) [32] demonstrated that if the tail behaviour of the distribution of atmospheric models is similar, those storm events could be aggregated and form a large storm event set in the framework of WiTRACK [36,37] along with a non-dimensional impact-related index, e.g., the storm severity index (SSI) [36]. The SSI was developed by Leckebusch et al. (2008) [36] to objectively quantify the severity of the storm based on its potential impact. SSI is defined as:

$$SSI = \sum_t \sum_k \left[\left(\max\left(0, \frac{v_{k,t} - v_{k,98}}{v_{k,98}} \right) \right)^3 \times A_k \right],$$

where $v_{k,t}$ is the wind speed of the kth grid box at time t, $v_{k,98}$ is the 98$^{\text{th}}$ percentile local climatological wind speed of the kth grid box, and A_k is the area dependent normalisation factor. By applying the Osinski–Thompson approach on the THORPEX Interactive Grand Global Ensemble (TIGGE) archive [38,39], Ng and Leckebusch (2021) [31] constructed the TIGGE Osinski–Thompson TC (TOT) event set for high impact TCs in the WNP. The TOT event set can be used for a more robust return period-return level estimation of TC-associated extreme wind at the local scale [31]. Here we define a regional SSI of an event as the accumulated SSI of a given event over the region of interest throughout the event lifetime.

In this study, we aim to address those challenges by answering two specific questions: (1) Can we construct trigger points of parametric typhoon insurance from a local perspective? (2) Can we improve the occurrence frequency estimation of TC-related extreme losses? The answers to these questions could optimise the post-disaster compensation and consequently speed up post-disaster recovery. In this study, an alternative method to construct trigger point for parametric typhoon insurance is proposed. A future development of such a trigger point is also discussed. Furthermore, we will show an approach to improve the estimated occurrence of TC-related losses on regional level using non-realised events from the TOT event set. The paper is organised as follows: Description of data and the underlying principle of our approach can be found in Section 2. Section 3 demonstrates an alternative approach to construct trigger points for parametric typhoon insurance. A procedure to improve the occurrence estimate of TC-related losses is shown in Section 4. Discussion and future improvement of the proposed approach is presented in Section 5. Conclusions can be found in Section 6. A list of acronyms is available in Appendix A.

2. Data and Methods

An impact-oriented windstorm tracking algorithm (WiTRACK [36,37]) is used for the identification of potential damage-relevant extreme windstorms based on local wind extrema above the 98$^{\text{th}}$ percentile of the local climatological wind speed. This approach has proved to be useful in assessing loss potentials due to European winter windstorms [35] and tropical cyclones (TCs) in the Western North Pacific (WNP) [40]. Befort et al. (2020) [40] showed that WiTRACK can identify approximately 90% of high impact TC-related events with more than 3000 million RMB losses in China. This demonstrates the suitability of WiTRACK in this study. The major difference between WiTRACK and other TC tracking algorithms is that WiTRACK identifies regions of extreme wind associated with storms rather than just the position of maximum wind or minimum sea level pressure. This forms

the so-called impact footprint of the storm. A detailed description of WiTRACK can be found in Leckebusch et al. (2008) [36], Kruschke (2015) [37], and Befort et al. (2020) [40]. The WiTRACK setting used in this study is identical to the setting that was used in Ng and Leckebusch (2021) [31]. Historical TC-related impact footprints are identified by applying WiTRACK on the 10-m wind of the fifth generation of atmospheric reanalysis European Centre for Medium-Range Weather Forecasts (ECMWF), i.e., ERA5 [41]. The ERA5 output that is used in this study has spatial resolution of $0.25° \times 0.25°$ and only time steps of 00, 06, 12, and 18 UTC are used.

The TIGGE data archive [38,39] is used in the construction of the TIGGE Osinski–Thompson TC (TOT) event set, as in Ng and Leckebusch (2021) [31]. Ensemble forecast data of four centres are used: China Meteorological Administration (CMA), ECMWF, Japan Meteorological Agency (JMA), and National Centers for Environmental Prediction (NCEP). A detailed description of the TOT event set can be found in Ng and Leckebusch (2021) [31]. The basic principle to construct the TOT event set is described as follows: (i) The high impact windstorm events in the ensemble forecast data is identified by WiTRACK. (ii) Windstorms that are similar to historical TC events are removed. (iii) Windstorms that do not have behavior as TCs, e.g., windstorms which are first identified far away from the tropics, or windstorms with erratic and short tracks, are removed. The TOT event set is shown to be realistic and has high information content [31]. This event set is suitable to use in evaluating the TC hazard in the WNP.

Historical TC information as reported by CMA, e.g., position and intensity, is obtained from the International Best Track Archive for Climate Stewardship (IBTrACS) v04r00 [42]. Historical in-situ surface wind data are obtained from the Integrated Surface Database (ISD) [43]. Only records in May to November are used as this is the period where TCs are the most likely to influence continental China. Provincial-level typhoon-related loss data from 1999–2018 are obtained from the China's Yearbooks of Meteorology (2000–2004) [44] and China's Yearbooks of Meteorological Disaster (2005–2019) [45]. Two types of loss entries are filtered out: (1) Entries with zero direct economic loss are removed, as the true loss is possibly non-zero, but still a small entry that is below the rounding or reporting threshold. (2) Loss events that involve multiple typhoons, namely Typhoons *Saola* and *Damery* (2012), Typhoons *Tembin* and *Bolaven* (2012), and Typhoons *Nesat* and *Haitang* (2017), have been removed to avoid further complexity in the analysis. While the main focus of this study is Guangdong, we have also extended our analyses to other coastal regions of continental China, namely Fujian, Zhejiang, and Jiangsu and Shanghai, to demonstrate the possible variations in the results. The geographic locations of these regions are shown in Figure 1. The number of observed loss events used in this analysis for Guangdong, Fujian, Zhejiang, and Jiangsu and Shanghai, are 63, 46, 42, and 19, respectively. Hazard footprint-based normalization [46] is applied to the historical loss data. The hazard footprint is defined as the impact footprint that is identified by WiTRACK. Gridded gross domestic product (GDP)–gross cell product (GCP) [47,48] is used to represent the spatial economic condition of the regions. The unit of GCP is 2005 USD in purchasing power parity. The reference year is chosen to be 2005. Data of administrative boundary of China is obtained from GADM database version 3.4.
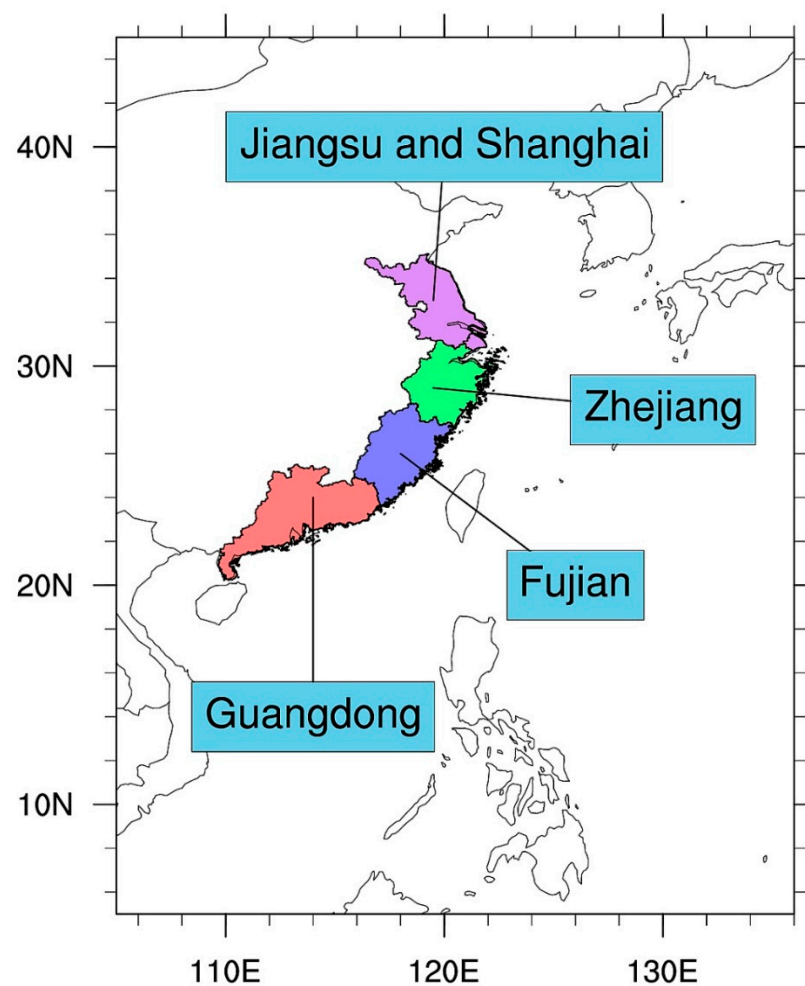
Figure 1. Geographic locations of the region of interest in this study.

3. Developing a Framework for Deriving Robust Trigger Points for Parametric Typhoon Insurance

As discussed in Section 1, the trigger points of parametric typhoon insurance, which are currently used, consist of two components: (i) the potential area of impact, which is represented by the distance between the centre of typhoon and the city; (ii) the severity of potential impact, which is represented by the intensity of the typhoon. Hereinafter, we refer to this type of trigger point as the storm-perspective trigger point (STP) as these are the variables which are used in typical meteorological storm reporting and the impact of the typhoon is implicitly included. STP has a strong assumption on the structure of tropical cyclones (TCs), however, the size and structure of typhoon varies even for typhoons with the same intensity [49]. This means the actual potential area of impact also varies for different typhoons. Consequently, using a fixed radius to represent the potential area of impact would lead to over- or under-estimation of actual extent of typhoon impact. Moreover, once a typhoon made landfall, the intensity of the typhoon would decay rapidly due to multiple physical processes, e.g., friction and reduction of surface evaporation [50]. Yet, those weakened typhoons, or TCs in general, could still cause significant damage to the inland regions due to lack of local impact experience in the past. On the other hand, coastal regions, which have more local impact experience, could benefit from their local investment to increase typhoon resilience. Thus, the potential TC-related impact would be reduced. These factors are not reflected by STP, which depends on the absolute intensity of a TC. In addition, TCs which did not make landfall with typhoon strength could also cause significant damage, e.g., Tropical Storm *Bilis* (2006).

An alternative approach to construct a trigger point for parametric typhoon insurance is to make use of local information. We refer to this type of trigger point as the local-perspective trigger point (LTP). In the framework of WiTRACK, only the top 2% of wind speed of the local climatological wind speed distribution is used as a proxy to quantify the region with TC-related damage potential. This implies that local assets would have the ability to withstand wind speed up to the top 2% of wind speed, which in turn represents the local TC hazard mitigation measures against extreme wind due to TCs. These measures would include early and effective warnings, increased public awareness and preparedness, and enhancement of infrastructure [51]. Consequently, the region covered by the impact footprint can be considered as the region with potential loss.

In this section, we assessed the differences between STP and LTP from the TC hazard impact perspective. First, we compared the frequency of occurrence of impact footprints, i.e., impact frequency, in the period 1999–2018, based on the potential impact area criteria of STP and LTP for four coastal regions of interest (Figure 2). The potential impact area of TC of STP was defined as the region within 106-km radius from a TC centre according to the CMA best track record for all TC intensity. In order to take into account that TCs with lower intensity could also cause damage, all TC intensities were used. A radius of 106-km was chosen to mimic the operational trigger point for Zhuhai city [9]. In all regions, the impact frequency was significantly higher when LTP was used in comparison to STP, in particular for further inland regions. This demonstrates the discrepancy in the trigger point construction from the pure meteorological perspective, which was represented by STP, and from the impact perspective, which was represented by LTP.

3.1. Triggering a Compensation: LTP versus STP

Within the LTP framework, parametric typhoon insurance could be triggered, if the grid boxes of the target region are covered by the impact footprint of TC as identified by WiTRACK. However, this does *not* imply the parametric typhoon insurance *has* to be triggered, as it would also depend on the local in-situ observations to verify the actual local impact of the TC. Consequently, the appropriate amount of compensation can be made to the insuree. This is analogous to the STP except using the local perspective. To demonstrate the importance of local information in triggering parametric typhoon insurance, the triggering consistency of STP has been evaluated from the local perspective. We make use of the results of a hindcast exercise, carried out by Swiss Re (Beijing) using experimental trigger points (ETPs). The Swiss Re hindcast exercise examined whether historical TC events in the period of 2011–2018 would trigger parametric typhoon insurance for the respective cities in Guangdong, if the ETPs were used. While the details of the ETPs design would be part of company internal procedures and proprietary products, the underlying principle of the construction of ETPs is similar to the design of STP as given in Section 1. The results of the hindcast exercise are either triggered or not triggered for cities in Guangdong. For those events that triggered a parametric typhoon insurance, we compare the wind speed of the in-situ weather stations with information from impact footprints covering the city. Therefore, we can examine whether ETPs are triggered consistently with reference to the LTP. The details of this demonstration are as follows:

(1) For the events in which ETP was triggered for a given city, the event associated impact footprint is used to determine whether the city is potentially impacted by the event, i.e., whether the impact footprint is found within the city.

(2) If the city is potentially impacted by the event, we extract the maximum in-situ observed wind speed within 24-h period (MW24), centered at the time of impact, of the observation station of the city. The 24-h period is used to minimise the likelihood of null observation at a given time.

(3) Consistency is evaluated by

    a. Whether the impact footprint can be found in the city

    b. Whether ETP is triggering consistently for a given MW24 of the in-situ observation station of interest.
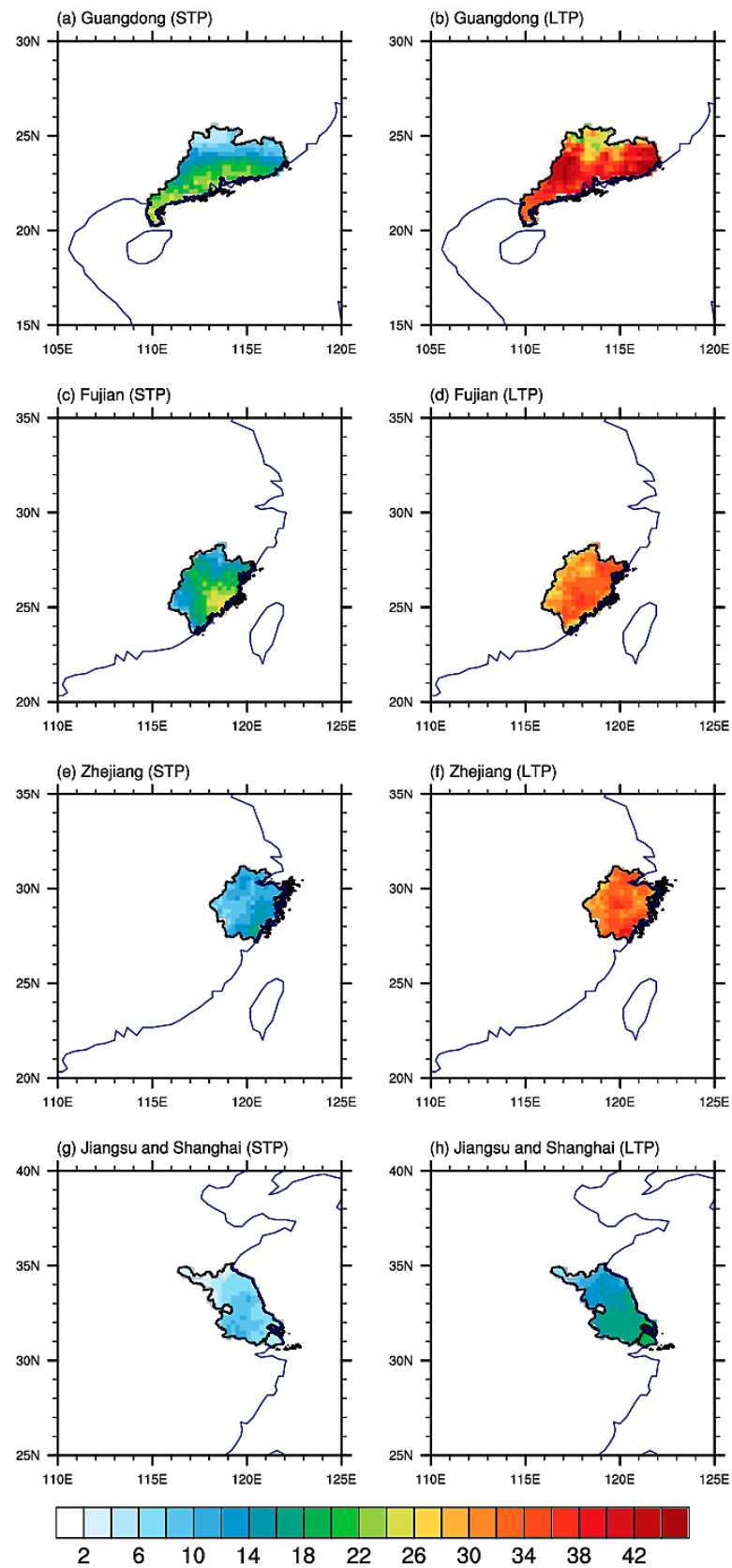
Figure 2. Impact frequency of TCs that caused direct economic loss. Units are total number of TC impact occurrences in the period 1999–2018. For four regions of mainland China: Guangdong, Fujian, Zhejiang, and Jiangsu and Shanghai (from **top** to **bottom**). Impact frequency based on STP (**a,c,e,g left column**) and LTP (**b,d,f,h right column**) are shown.

In this analysis, four cities of Guangdong, namely Shantou, Yangjiang, Shanwei, and Zhanjiang, are considered (c.f. Table 1 for the associate station and the geographic locations are shown in Figure 3). The results are shown in Table 2. Criteria (3a) is met 90% of all the cases where ETP was triggered. The exceptions are Tropical Storm *Pakhar* (2017) and Tropical Storm *Bebinca* (2018) for Yangjiang, where these two events are not identified by WiTRACK due to their low intensities. Therefore, no impact footprint is found for these two storms. Yet, these events led to large direct economic losses in Guangdong, 680 million RMB for Tropical Storm *Pakhar* (2017) and 1940 million RMB for Tropical Storm *Bebinca* (2018). A potential explanation is discussed in Section 5. Given that criteria 3a is satisfied for most cases where ETP was triggered, this shows the notion of LTP impact footprint is reliable in identifying the potential impact of typhoons. If ETP is consistently triggered, we would expect the ETP would *always* be triggered above a certain value of MW24. However, the consistency of ETP appears to be city-dependent (Table 2). In order to represent triggering consistency quantitatively, we define the trigger rate (TR) for a city as,

$$TR = \frac{\text{No. of events where ETP was triggered}}{\text{No. of events where ETP should have triggered based on MW24}} \qquad (2)$$

Table 1. Information of selected stations in Guangdong, Hong Kong, and Macau.

WMO Station ID	Name	Latitude (° N)	Longitude (° E)	Period	Province/Region
45004	Kowloon	22.312	114.173	1992–2001	Hong Kong
45005	Hong Kong Observatory (HKO)	22.3	114.167	1973–1996	Hong Kong
45007	Hong Kong Intl	22.309	113.915	1997–2018	Hong Kong
45011	Macau Intl	22.15	113.592	1973–2018	Macau
45032	Ta Kwu Ling	22.533	114.15	2002–2018	Hong Kong
45039	Sha Tin	22.4	114.2	2004–2018	Hong Kong
59087	Fogang	23.883	113.517	1973–2018	Qingyuan
59271	Huaiji	23.95	112.2	1973–2002	Zhaoqing
59278	Gaoyao	23.05	112.467	1973–2018	Zhaoqing
59287	Baiyun Intl	23.392	113.299	1973–2018	Guangzhou
59316	Shantou	23.4	116.683	1973–2018	Shantou
59317	Huilai	23.083	116.3	1973–2000	Jieyang
59462	Luoding	22.717	111.55	1973–2000	Yunfu
59478	Tai-shan	22.267	112.783	1973–2002	Jiangmen
59493	Baoan Intl	22.639	113.811	1973–2018	Shenzhen
59501	Shanwei	22.783	115.367	1973–2018	Shanwei
59658	Zhanjiang	21.217	110.4	1973–2018	Zhanjiang
59663	Yangjiang	21.867	111.967	1973–2018	Yangjiang
59664	Tian-cheng	21.517	111.3	1973–2002	Maoming
59673	Shangchuan Dao	21.733	112.767	1973–2018	Jiangmen

For Zhanjiang, the minimum MW24 of the corresponding in-situ observation station, in which ETP is triggered, is 9 m/s. Above this value, ETP is always triggered with the presence of an impact footprint in the city. Therefore, the TR for Zhanjiang is 1. For Yangjiang and Shanwei, where their minimum MW24 is 15 m/s and 10 m/s, respectively, ETPs are triggered relatively consistently with few cases which should be triggered for the given in-situ wind speed, but was not, for example, Typhoon *Mujigae* (2015) for Yangjiang and Typhoon *Mangkhut* (2018) for Shanwei. The value of TR for Yangjiang and Shanwei is 0.67 and 0.50, respectively. For Shantou, where the minimum MW24 is 4 m/s, ETP is not triggered consistently with the lowest TR of 0.33. It should be noted that the values of minimum MW24 for Yangjiang, Shanwei, and Zhanjiang, are close to the definition of so-called TC high wind, which is defined as the wind induced by a TC that exceeds 10.8 m/s [52,53]. This shows the above evaluation procedure for triggering consistency is reliable.
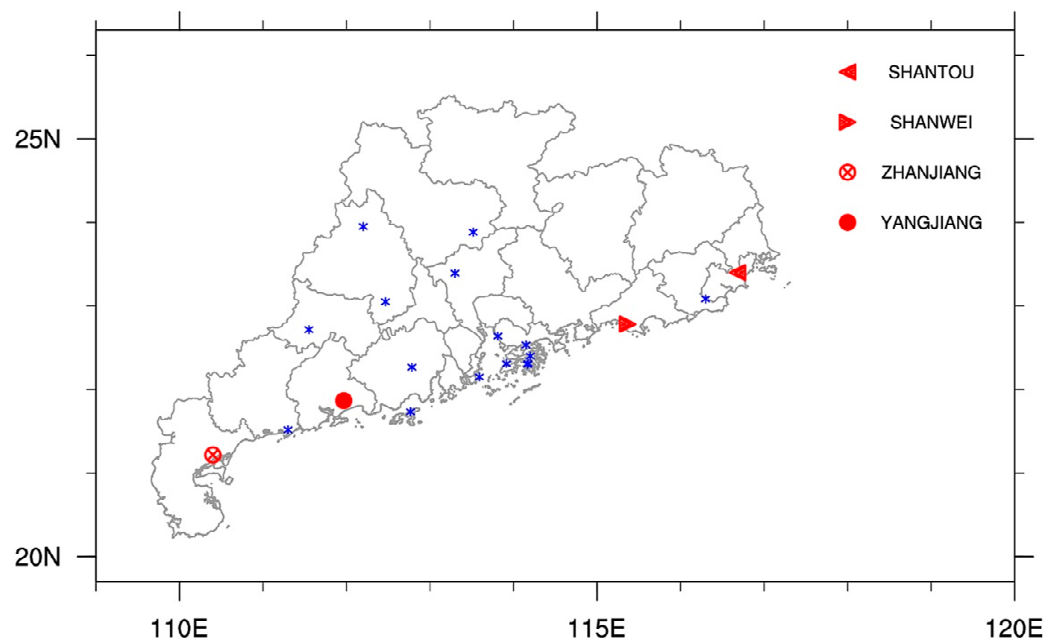
Figure 3. Location of selected stations in Guangdong, Hong Kong, and Macau in blue stars (data period, station ID, and exact positions are given in Table 1). The stations, which are selected for the analysis in Section 3.1 is shown in red (see legend).

Table 2. Examination of triggering consistency of ETP using results of Swiss Re hindcast exercise with reference to LTP (see Section 3.1 for details). ETP is triggered based on TC intensity as measured by CMA. Events, for which ETP is triggered, are in bold red. The numbers are the maximum in-situ observed wind speed within a 24-h period (m/s) centered at the time of impact (MW24), at the associated station of the given city. NV indicates no observed values. NF indicates no impact footprint covered the city. It can be seen, ETP is not consistently triggered for some cities for a given minimum MW24.

Year	Typhoon Name	Shantou	Yangjiang	Shanwei	Zhanjiang
2011	Nesat	NV	17	6	**21**
2012	Vicente	NV	**15**	9	5
2012	Kai-tak	NV	14	7	**19**
2013	Usagi	**10**	NF	**19**	NF
2013	Utor	4	**26**	6	8
2014	Hagibis	**5**	NF	6	NF
2014	Rammasun	NF	12	5	**17**
2014	Kalmaegi	5	14	10	**24**
2015	Linfa	**6**	11	**10**	NF
2015	Mujigae	5	16	6	**29**
2016	Nida	7	11	**13**	NF
2016	Haima	8	7	**17**	NF
2017	Mawar	**4**	NF	10	NF
2017	Merbok	5	NF	10	NF
2017	Hato	3	**15**	7	6
2017	Pakhar	NF	**NF**	NF	NF
2017	Khanun	6	13	7	**9**
2018	Mangkhut	5	**19**	18	8
2018	Bebinca	NF	**NF**	NF	NF

The reader should be aware that the results in the above analysis would also depend on the specific location of the station. For example, the range of in-situ observed MW24 for the Shantou station in the Swiss Re hindcast exercise is 3–10 m/s (Table 2). The range of wind speed appears to be too low in producing significant impact. Thus, even ETP has a

low TR in Shantou, it could be the case that the specific station is not located at the location where TC-related high wind speed would be observed during TC occurrence. This notion is supported by the large variations in the 20-year return level wind speed (Figure 4) of five in-situ stations in Hong Kong, namely, Kowloon, Hong Kong Observatory, Hong Kong Intl, Ta Kwu Ling, and Sha Tin. A potential approach to address this issue is discussed in Section 3.2.
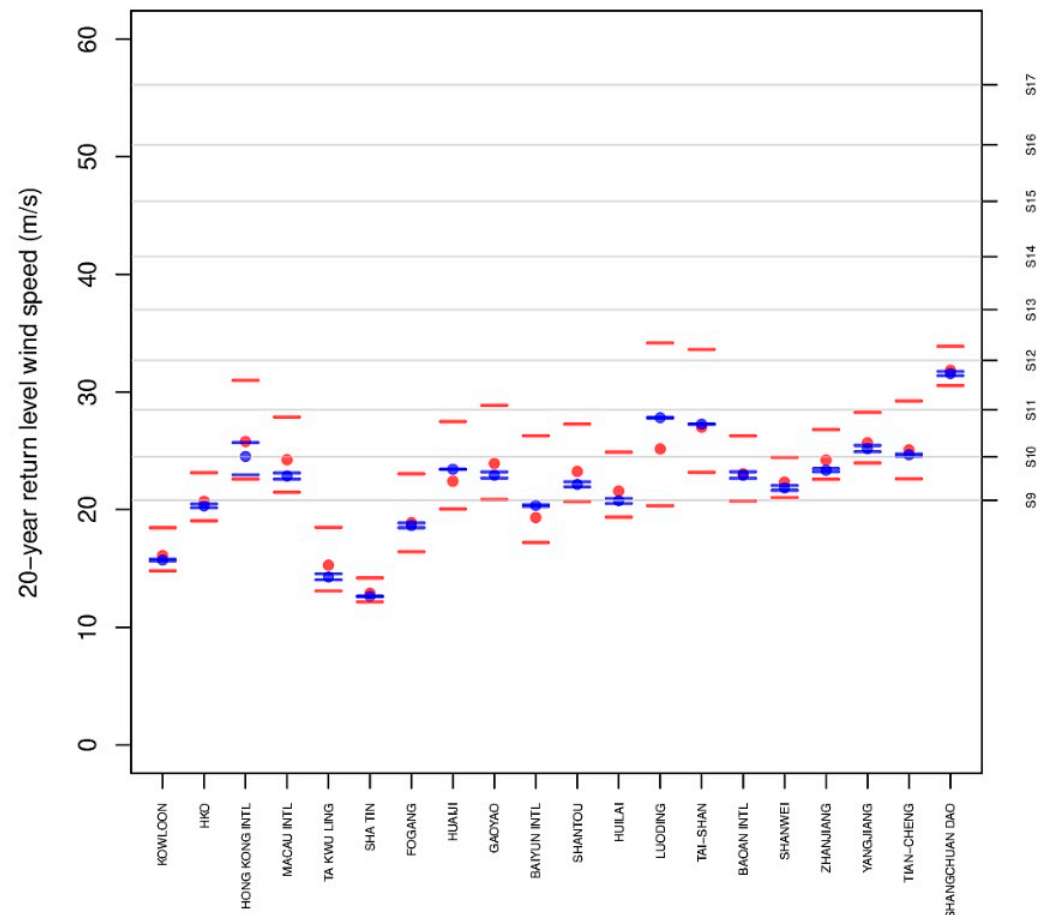

Figure 4. 20-year return level of selected stations in Guangdong, Hong Kong, and Macau, calculated from historical observations (red) and the TOT event set (blue). Bars and dots indicate the 95% confidence interval and estimates, respectively. Vertical axis on the right shows the corresponding category in the extended Beaufort wind scale.

3.2. Compensation Based on Event Occurrence in LTP

From the practitioner point of view, it is necessary to evaluate the likelihood of event occurrence. This is because this would affect the choice of trigger points which would consequently affect the pricing and potential compensation for the parametric typhoon insurance product. This implies, within the LTP framework, an accurate estimation of the occurrence of high impact TC events at the local scale is of necessity. In order to do so, there are two issues, which have to be overcome: (1) Due to the rarity of historical TCs, a robust estimation of extreme wind occurrence at the local scale based on historical observation is difficult; (2) As demonstrated in Section 3.1, suitable in-situ observations to detect relevant local impact might not yet exist.

The first technical issue can be overcome by using a method developed by Ng and Leckebusch (2021) [31]. The principle of the method is to increase the number of in-situ TC wind observations by using the TOT event set given that the stations have long consecutive records of at least 10 years. This method can increase the number of observations by up to 506 times more than the available historical observations in the in-situ observation stations

of Guangdong. Consequently, the occurrence of local extreme TC wind estimations can be improved. A workflow of this method is described as follows (also see Appendix B for schematic diagram for the workflow (Figure A1)):

(1)   Construct the TOT event set.
(2)   Select in-situ stations with long consecutive records, i.e., with at least 10 years of consecutive records, for reliable climatology.
(3)   For each selected station, we identify the closest grid boxes in the TOT event set (see Ng and Leckebusch (2021) [31] for detailed description).
(4)   Area scaled SSI of the relevant grid boxes are extracted
(5)   Mapped data from (4; storm severity index, SSI) to in-situ extreme wind observations using a transfer function e.g., quantile mapping.
(6)   Finally, the occurrence of extreme wind speeds is calculated using the threshold excess approach in the extreme value analysis.

Figure 4 shows the 20-year return level of in-situ wind speed at the selected stations (Table 1) in Guangdong calculated from historical observations and the values calculated using the approach based on the TOT event set described above. The estimates, which are derived based on the TOT event set have significantly smaller uncertainty estimates than their counterparts based on historical observations alone. Furthermore, these estimates based on the TOT event set are within the uncertainty range of the estimates derived from historical observations. This shows the added value of the approach. In addition, this approach can also be used to estimate a return level of a 100-year event, which is beyond the range of available historical observations. Consequently, decision and policy makers could also benefit from this approach by using the additional information in the development of policy for disaster risk reduction (DRR).

While the obvious solution to the second technical issue is to implement in-situ observation stations at the location where relevant local impact would be found, these new in-situ observation stations would not have long-term consecutive observations. As a result, it is difficult to have a robust estimation of extreme wind occurrence at the location of in-situ observation stations with short operational time. To overcome this issue, we can combine the above approach with the idea of spatial continuity via spatial interpolation. Figure 5 shows an example of a map of 20-year return level in Guangdong using the method above with natural neighbour interpolation [54].

In summary, we demonstrated the validity of the notion of local impact-oriented trigger point, i.e., LTP, in Section 3. We first compare the occurrence frequency of impact between the LTP framework and the traditional STP framework (Figure 2). It is found that the occurrence frequency of impact is higher in the LTP framework than in the STP framework. This shows the discrepancy in the trigger point construction from the pure meteorological perspective, i.e., STP, and from the local impact perspective, i.e., LTP. We then examine the triggering consistency of STPs from the local impact perspective. To achieve this, we used the results of hindcast exercise from a practitioner (Swiss Re) with ETP (a type of STP) and compared the in-situ observed wind speed around the time of impact for the cases where ETPs are triggered and the cases where ETPs are not triggered. It is found that there exists regional variability in the consistency of triggering compensation using ETP from the local perspective (Table 2). A mechanism of triggering compensation in the LTP framework has been proposed. Using the methods described above, practitioners could benchmark and fine-tune the parametric insurance trigger point from a local impact perspective. Consequently, a more "local-centric" parametric insurance trigger point can be developed with good sensitivity to the local impacts of typhoons. This could reduce the cases of over- or under-compensation and improve post-disaster recovery.
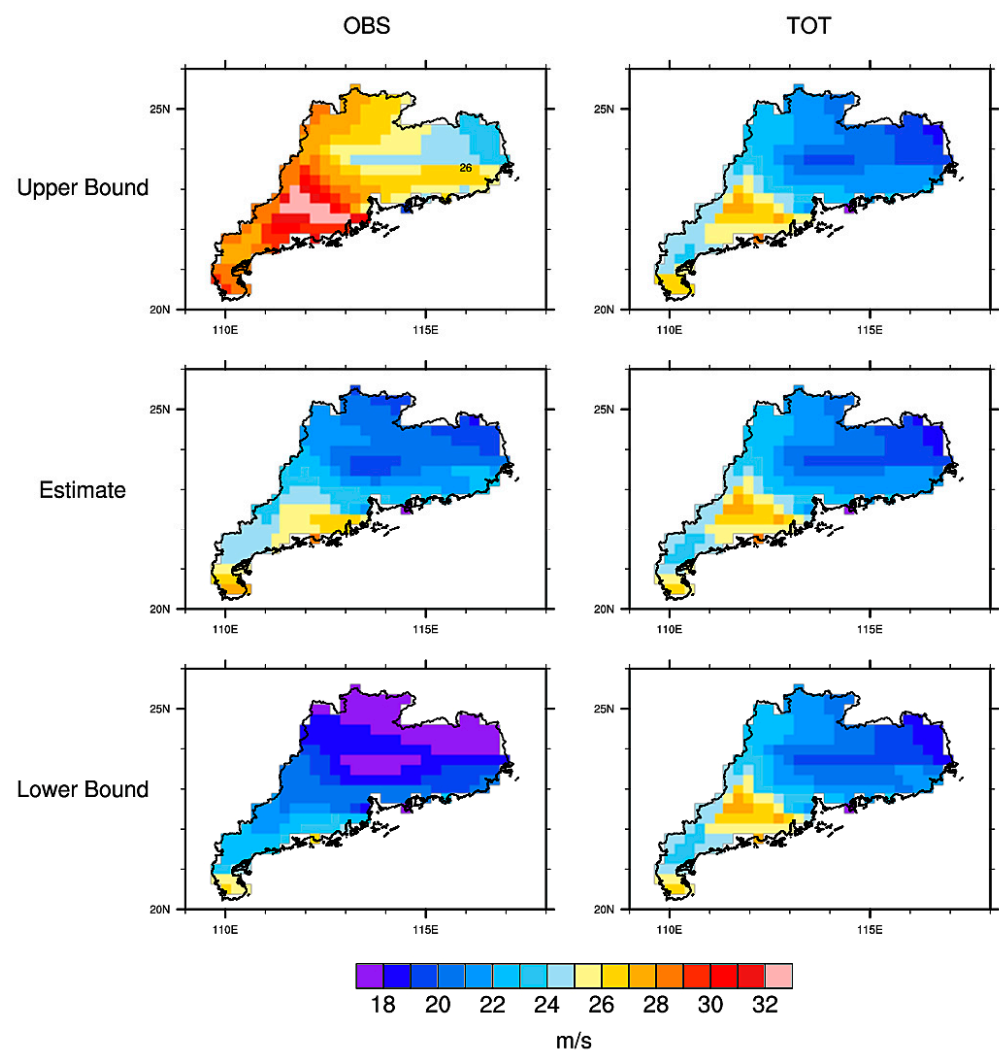
Figure 5. 20-year return level (in m/s) for Guangdong province derived using historical observations (OBS; **Left column**), and the TOT event set (TOT; **Right column**). The upper bound of the 95% confidence interval, estimate, and lower bound of the 95% confidence interval are shown in top, middle, and bottom rows, respectively.

4. Improving the Estimate of TC-Related Loss Occurrence on Regional Level

One crucial determination in the final choice of trigger points is their relation to expected losses per event. Ultimately, the fixation of the trigger point itself is a choice between the amount of compensation wished for (for multiple reasons e.g., economical, local cultural, ethical, demographic or, finally, political considerations) and the willingness of the participating parties to agree on the respective premium to be paid. The latter is again a consequence of the provider's estimate of the real risk of occurrence of an event of a certain strength and related loss characteristic. In this section, we thus analyse how far using the TIGGE Osinski–Thompson TC (TOT) event set and the approach as outlined above could lead to an improvement of estimates of tropical cyclone (TC)-related losses on regional level.

Due to the rarity of high impact TCs, there are very limited TC-related loss data and related meteorological information from historical records. In addition, accessibility and the necessary pre-processing procedure of the historical TC-related loss data of China could be a challenge [46]. Consequently, it is difficult to evaluate the occurrence frequency of a TC with a given potential (loss) impact of a region of interest solely based on historical events due to lack of sufficient available observations. Especially, for the very rare and extreme events, an accurate estimate would not be possible. To address this issue, we

can make use of the TOT event set, which contains large numbers of non-observed, but possible high impact TC events, with a 2-step procedure. First, from observed loss and meteorological data, we construct a loss-transfer function between regional storm severity index (SSI) and normalised loss for each of the four regions of interest. Second, the return period–return level estimate of TC-related loss events for the coastal regions of mainland China is calculated based on these loss-transfer functions and by utilising the TOT event set. The application of regional SSI in this procedure is of crucial importance: (1) Wind-based variables have been traditionally used in storm-related damage assessments [55–57]. (2) As discussed in Section 1, SSI is a non-dimensional quantity which allows us to construct a large storm event set by aggregating high impact TC events from different model outputs, e.g., the TOT event set, using the framework of WiTRACK. (3) By the construction of SSI (c.f. Equation (1)), it is a measure of meteorological severity of a TC with the consideration of the local resiliency to TC impact (c.f. Section 3). This means that the regional SSI can be seen as a measure of the overall meteorological impact of a given TC for a specific region. This procedure relies on the realism of the TOT event set, i.e., whether the TOT event set is consistent with historical observations. The TOT event has shown to be climatologically consistent, both spatially and temporally, with historical observations [31]. The validation of the consistency of the TOT event set and historical observations from the impact perspective can be found in Appendix C.

4.1. Estimating the Loss for Non-Realised Events: Regional SSI and Normalized Loss

While the TOT event set is shown to be a realistic representation of localized impact from the meteorological perspective (c.f. Appendix C), practitioners are more interested in the associated loss or socioeconomic impact. Since the latter are naturally not part of any meteorological ensemble predictions, it is required to attribute potential socioeconomic impact to non-realized TCs in the TOT event set by constructing a *loss-transfer function*, which links regional SSI and normalized loss (NLoss). It should be noted that the proposed method to construct the loss-transfer function is a principle way of solving the problem of loss attribution to non-realized events, based on historical provincial level losses. The ultimate quality of this loss-transfer function is not necessarily the relevant aspect of the proposed procedure of the estimation of TC-related loss occurrence. The best way of constructing such a loss-transfer function is beyond the scope of the current study and may be discussed in an independent study. Here we establish one way of deriving a loss-transfer function without loss of generality, i.e., modelling extreme losses. A brief discussion of potential improvement about the derivation of the loss-transfer function can be found in Section 5.

Ordinary least squares regression is used for deriving the loss-transfer function between regional SSI and NLoss based on the available loss information. Large regional differences in the loss-transfer functions are observed (Figure 6). This could be related to the regional differences in the socioeconomic development, as well as uncertainties in the in-situ practice loss assessment shortly after the respective events or based on a certain random element in the realization of losses from event to event. The relevance of a variable influence of extreme precipitation on event losses are also to be considered as a potential factor, we refer the reader to Section 5 for the discussion of further improvements.

Due to the shortage of historical TC-related loss data and the associated meteorological observations especially for the extremely high impact events, the gradient of the resultant regression fits (hereinafter the *optimistic scenario* (black lines in Figure 6)) are very gentle, and the extremely high impact events could be interpreted as outliers for Guangdong, Fujian, and Zhejiang, based on this view. To our expert judgement and for the sake of clarity in the context of this study, we conclude the optimistic scenario for Guangdong, Fujian, and Zhejiang, would not be suitable to be used as they do not model the extreme tail of the loss distribution well. As shown later, using the optimistic scenario as loss-transfer functions would lead to severe underestimation of the occurrence frequency of events associated with extreme losses, and would thus lead to unrealistic loss occurrence estimates.
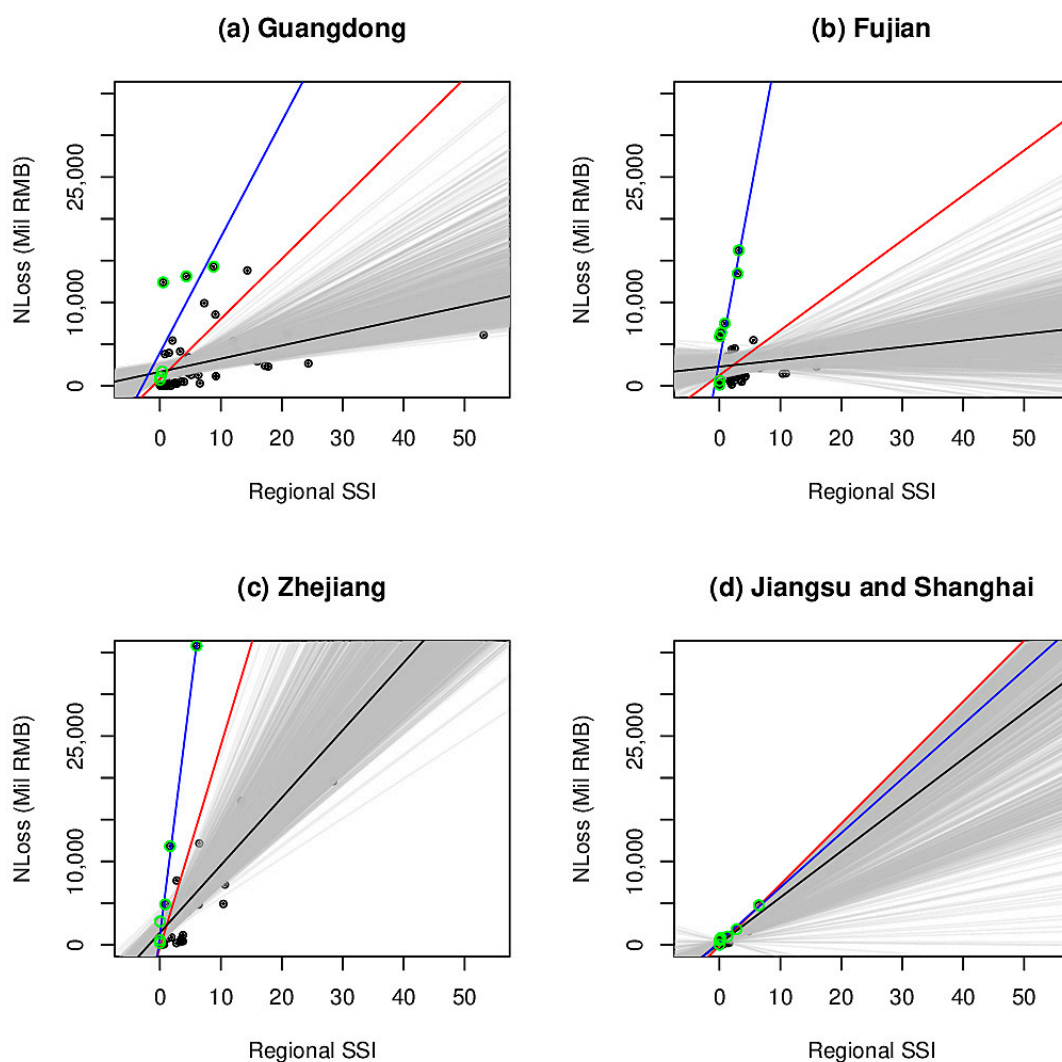
(a) Guangdong

(b) Fujian

(c) Zhejiang

(d) Jiangsu and Shanghai

Figure 6. Relationship between regional SSI and NLoss of TC events in the period of 1999–2018. Black lines indicate the regression lines derived using the full data set (black dots). Grey lines indicate the regression lines of the sensitivity experiment. Red lines indicate the regression line with the steepest slope in the sensitivity experiment. Blue lines indicate the maximum potential loss which are derived using selected data points as indicated by green dots. See main text for detailed explanation.

Consequently, we performed systematic tests to evaluate the sensitivity of the regression fit with respect to the few available loss data. For each region, resample data sets, which have an identical number of data entries as the original data set, are constructed using bootstrap random sampling (with replacement), and then a regression fit is calculated for each of the resample data sets (grey lines in Figure 6). This has been repeated 1000 times for statistical robustness. The regression fit is very sensitive to the data entries as demonstrated by the large spread of regression fits from the sensitivity test. This is related to rare occurrence of TCs especially for high impact TCs as well as the potential uncertainty in the loss data. The regression fits with the steepest slope in the sensitivity experiment, hereinafter the *pessimistic scenario* (red lines in Figure 6), appear to be a better loss-transfer function than the optimistic scenario for the extreme events for Guangdong, Fujian, and Zhejiang. This is because the pessimistic scenario leans toward the extreme events and away from the unrealistic loss-transfer function discussed above, i.e., the optimistic scenario.

An alternative approach to construct a loss estimate for non-realized events, is to focus on the **maximum potential loss** for a given regional SSI (blue lines in Figure 6). The

maximum potential loss is derived by first reordering all data entries by its SSI in ascending order. Then, if the NLoss value of the current data entry is larger than all previous records, this data entry is kept. This process is repeated for all data entries and the resultant set of data entries are shown in green circle in Figure 6. The maximum potential loss is then represented by the ordinary least squares regression between regional SSI and NLosss of those remaining data entries. The gradient of the maximum potential loss is the steepest slope in all regression lines for Guangdong, Fujian, and Zhejiang. The use of the maximum potential loss fit will stand for a very loss-sensitive perspective for non-realized events, i.e., would probably lead to an over-estimation of losses for extreme events. It could thus be seen as the *worst-case scenario* on potential losses due to the high sensitivity to the regional storm severity.

The loss-transfer functions for the optimistic, pessimistic, and the worst-case scenarios for Jiangsu and Shanghai are special cases in comparison to other regions, as they have similar steepness. Obviously, there is less variation in the loss data and consequently the loss-transfer function of the optimistic scenario is comparatively a "well-fitted" function for the historical loss data. Thus, the results for Jiangsu and Shanghai can be used as a *scenario-independent* evaluation of our proposed procedure.

In our following pilot demonstration, we will estimate the occurrence frequency of extreme losses based on different sensitivity scenarios of the loss-transfer function, i.e., the **optimistic** (black line in Figure 6), the **pessimistic** (red line in Figure 6), and the **worst-case** scenarios (blue line in Figure 6), using the TOT event set of non-realized, but physically possible, events. By doing so, we provide uncertainty ranges for extreme event occurrence estimates, taking into account that the applied loss-transfer function may be far from perfect, but still allows us to assess on three different risk sensitivities without any loss of generality.

4.2. Developing Alternative Views on the Real Risk of Losses from Severe Typhoons: Return Period-Return Level Estimation

This section will demonstrate how an alternative view on trigger points could be derived from the set of non-realized events. As discussed in Section 4.1, the true return period-return level estimation would depend on the true link between historical loss and the associated meteorological impact in the respective region, which is beyond the scope of this study. Return period–return level estimation is done using the R package *extRemes* [58] based on the threshold excess approach. For convenience, we normalized the NLoss with the largest NLoss (in unit of millions of RMB) observed in the respective regions, i.e., 14,281 Million RMB for Guangdong (Typhoon *Mujigae* 2015), 16,224 Million RMB for Fujian (Typhoon *Dan* 1999), 35,810 million RMB for Zhejiang (Typhoon *Fitow* 2013), and 4740 million RMB for Jiangsu and Shanghai (Typhoon *Matsa* 2005).

The return period–return level estimations based on historical observations (green lines), the optimistic scenario (black lines), the pessimistic scenario (red lines), and the worst-case scenario (blue lines), are shown in Figure 7. First, for all regions, the return period–return level estimations based on historical observations has a large uncertainty range in comparison to the other estimations, regardless of the choice of the loss-transfer function. It has to be noted that there are not enough extreme TC-related regional loss events in the historical observations, i.e., only a few data entries are used in the return period–return level estimation when historical observations are used. This is because the available loss data of the regional resolution is only available for the 20-year period. Consequently, the estimation based on historical observations (green lines in Figure 7) might not be fully reliable and may be far off from the real occurrence frequency of events of such impact. The uncertainty ranges and estimates, which are derived from all scenario based on the TOT event set, i.e., the optimistic, the pessimistic and the worst-case scenarios, have smaller uncertainty than estimation based on historical observations, as verified by the scenario-independent estimates of Jiangsu and Shanghai (Figure 7d). This is obviously due to the fact that much more data are available from the TOT event set, i.e., 16,144 for Guangdong, 9066 for Fujian, 5973 for Zhejiang, and 2412 for Jiangsu and Shanghai, the key strength

of this approach. These fits consequently profit from the existence of more events at the tail of the severity distribution, such that the relevant part for high-profile losses can be investigated in more detail and more reliably. Second, the estimated curves derived from the historical observations for all regions are relatively flat in comparison to the estimations from the TOT event set based on the loss-transfer function of the pessimistic scenario and the worst-case scenarios. This is linked to the number of observed extremes available in the distribution of the respective set of observations as demonstrated by the estimates derived from the optimistic scenario for Guangdong, and Fujian. Since the slope of the loss-transfer functions of the optimistic scenario for Guangdong, and Fujian is very gentle, in order to reach extremes NLoss, for example NLoss above 10,000 Mil RMB, the value of regional SSI must be extremely large. Consequently, even for the TOT event set, few events would have such a value of regional SSI, and thus the available number of data entries for the return period-return level estimation is low. The steepness of the uncertainty ranges and estimates that are derived from the TOT event set using different scenario loss-transfer function is controlled by the sensitivity of the loss-transfer function with respect to regional SSI, i.e., the gradient of the loss-transfer function (Figure 6). Nevertheless, such sensitivity does not undermine the general principle of the proposed procedure in improving the occurrence frequency estimation of extreme TC-related losses as demonstrated in Figure 6d.
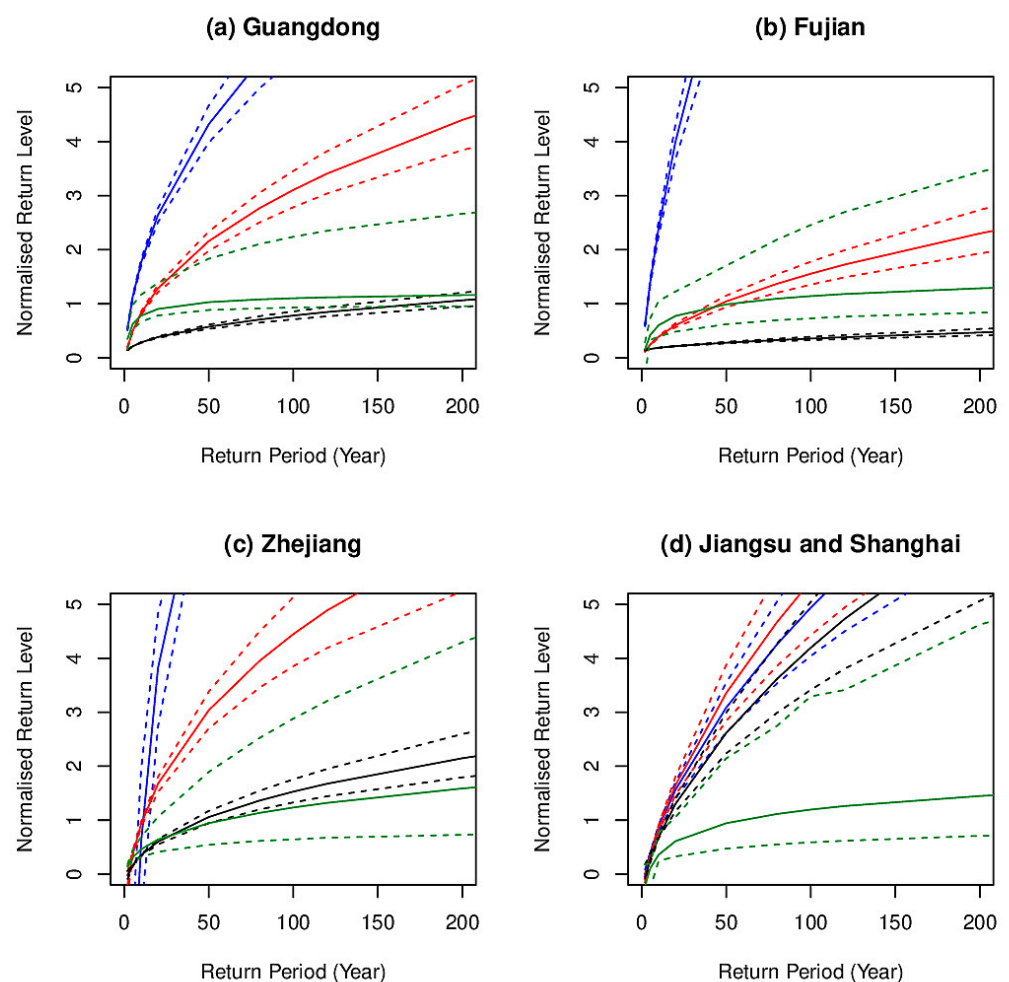

Figure 7. Return period-return level estimation calculated using historical observations (green solid: estimate; green dashed: 95% confidence interval), and using the TOT event set based on the optimistic scenario (black solid: estimate; black dashed: 95% confidence interval), the pessimistic scenario (red solid: estimate, red dashed: 95% confidence interval) and the worst-case scenario (blue solid: estimate, blue dashed: 95% confidence interval). Return level is normalised by the maximum NLoss of the respective regions (see main text).

As shown in Table 3, the return period estimates of TC-related losses calculated based on historical observations contain large uncertainty. This is always the case for the return period estimates for the highest impact TCs in the respective regions, for example, the estimated return period for Typhoon *Mujigae* (2015) in Guangdong has uncertainty range from 6 to more than 800 years. From the hazard assessment point of view, this does not provide any useful information as the uncertainty range is too large. On the other hand, the return period estimates calculated based on the TOT event set, i.e., the optimistic, the pessimistic, and the worst-case scenarios, provide much smaller uncertainty ranges. The estimates based on the optimistic scenario appears to be unrealistic, as it is highly unlikely that one would observe three roughly 150-year events within a five year period, i.e., Typhoon *Usagi* (2013), Typhoon *Mujigae* (2015), and Typhoon *Hato* (2017) (Table 3). On the other hand, the estimates based on the pessimistic scenario and the worst-case scenario appear to be more realistic.

Table 3. Estimated return period (in years) for the top three highest impact events for the respective regions derived from Figure 7. The numbers in the bracket indicate the lower and upper bounds of the uncertainty range.

Region	Year	Typhoon Name	Historical	Optimistic Scenario	Pessimistic Scenario	Worst-Case Scenario
Guangdong	2015	Mujigae	43 (6–>800)	176 (138–230)	14 (13–15)	4 (4–5)
	2013	Usagi	35 (5–255)	164 (129–212)	13 (12–14)	4 (4–4)
	2017	Hato	23 (5–84)	146 (115–188)	12 (11–13)	4 (4–4)
Fujian	1999	Dan	53 (9–>800)	>800 (676–>800)	47 (41–57)	4 (3–4)
	2016	Meranti	27 (7–192)	717 (475–>800)	35 (31–41)	3 (3–3)
	2005	Longwang	6 (3–17)	192 (147–268)	13 (12–14)	<2 (<2–<2)
Zhejiang	2013	Fitow	59 (18–>800)	46 (40–57)	11 (10–12)	11 (8–15)
	2004	Rananim	15 (7–52)	18 (16–20)	7 (6–7)	10 (8–14)
	2012	Haikui	11 (6–36)	15 (14–17)	6 (6–7)	10 (8–14)
Jiangsu and Shanghai	2005	Matsa	60 (18–>800)	15 (14–17)	12 (11–13)	12 (11–13)
	2005	Khanun	11 (7–34)	6 (5–7)	6 (6–6)	5 (5–5)
	2012	Haikui	10 (6–24)	6 (5–7)	5 (5–5)	5 (5–5)

We may capitalize on the estimates from these two scenarios by combining the uncertainty ranges of both estimates. For example, based on this view, the estimated return period of losses associated with Typhoon *Mujigae* (2015), Typhoon *Usagi* (2013), and Typhoon *Hato* (2017) are roughly within 4 and 15 years. Given that these three typhoons occurred within a 20 year period (1999–2018) and that their associated NLoss are similar, i.e., 14,281 million RMB for Typhoon *Mujigae* (2015), 13,822 million RMB for Typhoon *Usagi* (2013), and 13,118 million RMB for Typhoon *Hato* (2017), we would expect these TC-related losses would have a similar return period from the impact point of view. Consequently, the return period estimations calculated using the TOT event set based on the pessimistic and worst-case scenarios appear to be more realistic than the estimations calculated using the historical event set. This shows the use of the TOT event set would provide useful information for hazard assessment. Similar conclusions can be reached for other regions (Table 3). To further demonstrate the usefulness of this approach, we estimate a potential impact of a 100 year event using the pessimistic scenario for different regions. It is estimated that the potential impact of a 100 year event would have roughly 3.1 times the most impactful event so far in Guangdong, namely Typhoon *Mujigae* (2015). For Fujian, a 100 year event would cause roughly 1.6 times more loss than Typhoon *Dan* (1999). The potential impact of a 100 year event would lead to 4.4 and 5.4 times more losses than the highest impact events in Zhejiang–Typhoon *Fitow* (2013), and Jiangsu and Shanghai–Typhoon *Matsa* (2005), respectively.

5. Discussion on Further Improvements and Applications of Our Approach

The major advantages of using the TIGGE Osinski–Thompson TC (TOT) event set in improving parametric typhoon insurance, as demonstrated in Sections 3 and 4, are (1) much fewer assumptions would be needed during the construction of event set and analysis while maintaining the physicalness of the results as the historical observations can be treated as a subset of the TOT event set [31]; (2) it enables the construction of trigger point from the local point of view, i.e., local-perspective trigger point (LTP). The notion of LTP has been shown to be realistic, as shown in Section 3.1. Furthermore, the TOT event set has been shown to be useful to reduce the uncertainty in return period–return level estimation of tropical cyclone (TC)-related losses for regions of interest (Section 4.2). In this section, we discuss the current limitations and potential improvement of LTP from the disaster risk reduction (DRR) perspective as well as for further applications.

(1)   In the current realization of this approach, we use a wind-based severity proxy to assess the overall damage potential and not only from wind, but including those forced e.g., by the flood hazard. The principle suitability for TC impact assessment has been shown by Befort et al. (2020) [40]. However, the use of a wind-based variable alone is an over-simplification in quantifying the potential impact of TCs. This could lead to two issues: Weak TCs with high socioeconomic impact are not included in the current analysis because they are not identified by WiTRACK as events with impact potential due to their low wind speed, for example, Tropical Storm *Pakhar* (2017) and Tropical Storm *Bebinca* (2018) (Table 2). This is aligned with the current parametric typhoon insurance policy, as weak TCs should not trigger compensation. Yet, some of these events have caused severe impact in China because of non-wind induced damage.

(2)   The socioeconomic impact of TCs is underestimated if a wind-based metric is solely used, as demonstrated by the outliers, which can be interpreted by the events which are located far away from the fit of the optimistic scenario (black line in Figure 6). These events have comparatively low regional SSI, but the corresponding NLoss is high. The impact of these events is often related to the extreme rainfall and other secondary hazards (e.g., storm surge, and landslide). Tropical Storm *Bilis* (2006) and Typhoon *Hato* (2017), which are two of the outliers in Figure 6a, are good examples. Tropical Storm *Bilis* (2006) made landfall without typhoon strength. The intensity of Tropical Storm *Bilis* (2006) was low throughout its lifetime, but it produced a large amount of precipitation over land. This is because as Tropical Storm *Bilis* (2006) made landfall at Fujian, it weakened; however, unlike typical TCs making landfall over mainland China, Tropical Storm *Bilis* (2006) did not move northward, but slowly westward and later southwestward. This was due to a persistent strong anticyclone over north-central China and westward extension and intensification of the WNP subtropical high [59]. Combining with the abundant moisture over southern and central China, the strong monsoonal flow at 850 hPa, and lifting of the lower atmospheric flow, Tropical Storm *Bilis* (2006) produced extensive and persistent precipitation over southern China [59]. According to CMA [60], Typhoon *Hato* (2017) made landfall in Guangdong with a typhoon strength of at least (45 m/s). The extreme rainfall associated with Typhoon *Hato* (2017) led to flash flooding and increased water level for several rivers. Due to the astronomical high tide, the storm tide associated with Typhoon *Hato* (2017) surpassed historical record for six tidal wave-observing sites in the Pearl River Delta Estuary [60] and the return period was estimated to be above 100 years [61].

These issues are related to the fact that current trigger points of parametric typhoon insurance, both storm-perspective trigger point (STP) and LTP, depend solely on wind speed, which does not in all cases account for the total impact of typhoons. This is understandable, because the typhoon definition is defined based solely on wind speed of the TC, i.e., maximum sustained winds at the center of the TC [1]. From the DRR perspective, any risk mitigation tool, e.g., a parametric insurance, should account for all

TC-related impacts. This would motivate the development of a general TC-parametric insurance, which could capture the compound nature of TC hazards. This is an ongoing research topic to include other meteorological variables, representing direct or indirect TC-related hazards, in the construction of an objective hazard-focused compound storm index. Once successfully developed, such a product could be applied in a comprehensive TC parametric insurance. Furthermore, an objective compound storm hazard index could also influence the construction of any loss-transfer function.

The new approaches, which we have presented in this study, can be used in a wider context of TC impact assessment. Many studies investigated the changes in TC-related losses on climate time scales around the world using historical data [46,62–67]. Since the principle of our approaches is general, they can be used for an in-depth analysis on the potential global risk of TCs on the climate time scale. The results would further improve our capacity in DRR for the future climate.

6. Conclusions and Summary

This study provides possible solutions to the two major challenges in developing optimal parametric typhoon insurance by using the physically consistent TIGGE Osinski–Thompson TC (TOT) event set and the local-perspective trigger point (LTP) framework. The main findings are summarized as follows:

(1) Storm-perspective trigger point (STP) has been compared with LTP, and we demonstrate that tropical cyclone (TC)-related impact frequency is based on the LTP framework is higher than the classical STP (Figure 2).

(2) Using the local perspective provided by the LTP, the triggering consistency of an experiment STP developed by Swiss Re, i.e., experimental trigger point (ETP), has been evaluated. It is found that there exists a regional variability in the triggering consistency of the ETP. This also demonstrated the potential over- and under-compensation issue in the classical STP.

(3) A mechanism for triggering compensation in the LTP framework has been proposed. In-situ wind observation can be used as a trigger point rather than the intensity of the typhoon as estimated by satellite technique. Furthermore, under the LTP framework and the TOT event set, the trigger point can be optimized. This would improve the sensitivity of parametric typhoon insurance from the local perspective.

(4) A method to improve the estimate of TC-related loss occurrence on a regional level has been proposed. This is achieved with a two-step procedure: (i) development of a loss-transfer function between observed normalized losses and regional SSI; (ii) Using the loss-transfer function attribute losses to the TOT event set, and the return period-return level calculation is done using the TOT event set.

Potential improvement of our approach has also been discussed. We emphasize that from the disaster risk reduction (DRR) perspective, a risk mitigation tool for TCs should account for all TC-related impact. This also motivates the necessity of the development of a general TC compound hazard risk parametric insurance rather than a wind-based only parametric typhoon insurance. This would further strengthen the resiliency of coastal cities against TCs. Future work would focus on the development of compound TC hazard parametric insurance based on the LTP framework.

In summary, this study demonstrates (1) a new approach to construct trigger points from the local impact perspective, and (2) the historical record of TCs is insufficient for developing a true picture of risk at the local level; however, a more realistic occurrence of TC-related losses can be examined using the TOT event set. These new approaches provide an alternative view on trigger points of parametric typhoon insurance and practitioners may use these new approaches to benchmark their existing trigger points as an important aspect of the capability to understand the risk of typhoon induced losses.

Appendix A. List of Acronyms

Table A1. List of acronyms.

Acronyms/Term	Description
CDF	Cumulative distribution function
CMA	China Meteorological Administration
DRR	Disaster risk reduction
ECMWF	European Centre for Medium-Range Weather Forecast
EPS	Ensemble prediction system
ETP	Experimental trigger point
GCP	Gross cell product
GDP	Gross domestic product
IBTrACS	International Best Track Archive for Climate Stewardship
ISD	Integrated Surface Database
JMA	Japan Meteorological Agency
LTP	Local-perspective trigger point
MW24	Maximum in-situ observed wind speed within 24-h period centred at the time of impact, of the observation station of the city
NCEP	Nation Centers for Environmental Prediction
NLoss	Normalized loss
SSI	Storm severity index
STP	Storm-perspective trigger point
Swiss Re	Swiss Reinsurance Company Ltd.
TC	Tropical cyclone
TIGGE	THORPEX Interactive Grand Global Ensemble
The TOT event set	The TIGGE Osinski–Thompson TC event set
TR	Trigger rate
WMO	World Meteorological Organization
WNP	Western North Pacific

Appendix B. Workflow of the Application of the TOT Event Set in Deriving Local Return Levels
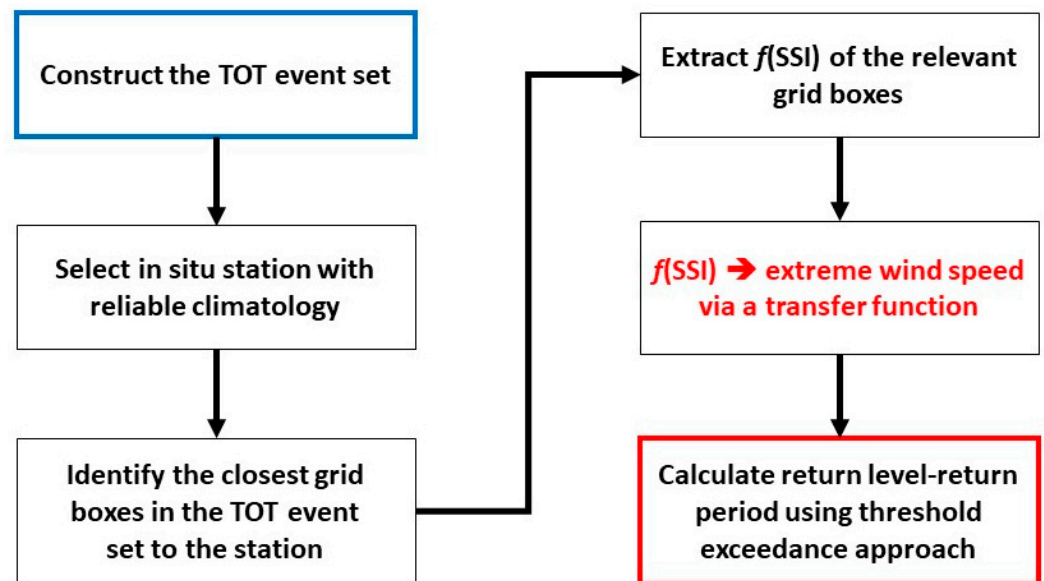

Figure A1. Workflow of the application of the TOT event set in deriving local return levels.

Appendix C. Validation of the Consistency of the TOT Event Set and Historical Observations from the Impact Perspective

To demonstrate the TOT event set is consistent with historical observations from the local impact perspective, we compare the cumulative distribution function (CDF) of regional SSI between historical observations and 100,000 random subsets of the TOT event set (Figure A2). These random subsets of the TOT event set are constructed using bootstrap random sampling (with replacement) and they have the same number of observations as the historical observations in the respective region. As shown in Figure A2, the CDFs of the historical observations (red lines) are placed within the range of the CDF of subsets of the TOT event set. This shows the historical observations are one of the possible realisations in the TOT event set. Consequently, the TOT event set is well-suited for our impact analysis.

As a technical note, there are historical TCs with non-zero regional SSI but having no documented TC-related loss (hereinafter non-loss events). The majority (>80%) of these non-loss events have regional SSIs of less than 0.1. A possible explanation is that the losses of these events could be smaller than the reporting threshold of loss records. These non-loss events are not included in the above calculation (Figure A2) neither in the calculation of return period-return level estimation using historical loss data in Section 4.2. In order to mimic the existence of non-loss events in the TOT event set, we have randomly selected events with regional SSI between 0 and 0.1 to be excluded from our calculations. The ratio of exclusion is the same as the ratio of non-loss events to all events in the historical record. For our analysis in Section 4.2, the random exclusion of events does not have any impact on the return period-return level estimation because the excluded events are eliminated by the threshold that is used in the threshold excess approach for return period-return level estimation [58]. If the threshold selected for the return period-return level estimation is low, it would be necessary to evaluate the influence of random selection of events with regional SSI of less than 0.1.
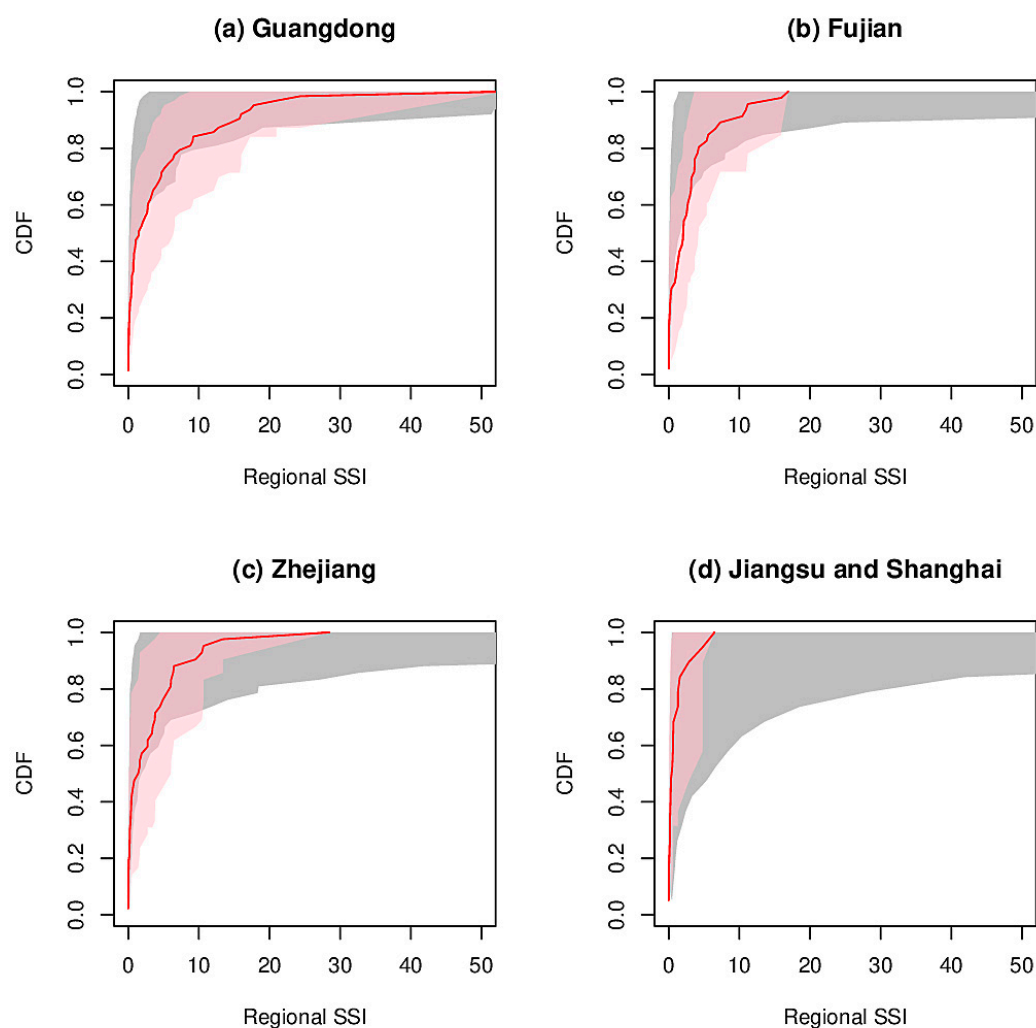
Figure A2. The cumulative distribution function (CDF) of the regional SSI in historical observations (red lines) for (**a**) Guangdong, (**b**) Fujian, (**c**) Zhejiang, and (**d**) Jiangsu and Shanghai. The grey areas indicate the range of CDF of the regional SSI in the 100,000 subsets of the TOT event set. The pink areas indicate the internal variability of the CDF of historical observations which are derived by bootstrap resampling with replacement.

References

1. WMO. *Typhoon Committee Operational Manual. Tropical Cyclone Programme Report No. TCP-23*; World Meteorological Organization: Geneva, Switzerland, 2019.
2. CMA. Tropical Cyclone Damages in China under Global Warming. Available online: http://www.cma.gov.cn/en/SciandTech/2 01307/t20130709_218970.html (accessed on 16 June 2021).
3. CMA. Member Report. In Proceedings of the 13th Integrated Workshop ESCAP/WMO Typhoon Committee, Chiang Mai, Thailand, 4–8 November 2018; p. 36.
4. UNISDR. *Sendai Framework for Disaster Risk Reduction 2015–2030*; UNISDR: Geneva, Switzerland, 2015.
5. Ye, T.; Wang, Y.; Wu, B.; Shi, P.; Wang, M.; Hu, X. Government Investment in Disaster Risk Reduction Based on a Probabilistic Risk Model: A Case Study of Typhoon Disasters in Shenzhen, China. *Int. J. Disaster Risk Sci.* **2016**, *7*, 123–137. [CrossRef]
6. Lemcke, G. A Resilient World: NatCat Parametric Insurance Solutions for China's Provincial Government. Available online: https://www.swissre.com/dam/jcr:54a44b69-a85f-4300-80ab-abfbaa51c139/GerryLemcke_+NatCat+parametric+insura nce+solution+for+Guangdong.pdf (accessed on 13 September 2020).
7. China-insurance.com. Guangdong Catastrophe Insurance Has Covered 18 Prefectures and Cities across the Province and Achieved a Total Premium Income of Approximately 800 Million Yuan in Five Years. Available online: http://www.china-insura nce.com/yc/20210818/59393.html (accessed on 22 October 2021). (In Chinese)
8. Ding, Y. A Summary of the Pilot Projects of Catastrophe Insurance in China. Available online: http://pl.sinoins.com/2017-11/0 9/content_246910.htm (accessed on 22 October 2021). (In Chinese)

9.	Zhuhai Financial Work Bureau. Zhuhai Financial Work Bureau Contract of Year 2021 Zhuhai City Catastrophe Index Insurance Purchase Project. Available online: https://gdgpo.czt.gd.gov.cn/uploader-gpms/upload/commoninfo/2021/5/31/1622455974 783_4492.pdf (accessed on 7 July 2021).

10.	Dvorak, V.F. Tropical Cyclone Intensity Analysis and Forecasting from Satellite Imagery. *Mon. Weather Rev.* **1975**, *103*, 420–430. [CrossRef]

11.	Ying, M.; Zhang, W.; Yu, H.; Lu, X.; Feng, J.; Fan, Y.; Zhu, Y.; Chen, D. An Overview of the China Meteorological Administration Tropical Cyclone Database. *J. Atmos. Ocean. Technol.* **2014**, *31*, 287–301. [CrossRef]

12.	Guangdong Provincial Government Procurement Center. Guangdong Province 2021–2023 Catastrophe Insurance Service Procurement Project Subpackage 3 Won the Bid Announcement, and Subpackage 1 and Subpackage 2 Failed Announcement. Available online: http://www.gdgpo.gov.cn/showNotice/id/2d908ce5766188ed01766525aa2b01c9.html (accessed on 22 October 2021). (In Chinese)

13.	China Government Procurement Network. Announcement on the Results of the 2021–2023 Catastrophe Insurance Service Procurement Project in Yangjiang City and Chaozhou City. Available online: http://www.ccgp.gov.cn/cggg/dfgg/zbgg/20210 5/t20210511_16267230.htm (accessed on 22 October 2021). (In Chinese)

14.	He, K. Zhuhai Catastrophe Index Insurance Has Been Implemented, and the Maximum Compensation Can Be 390 Million Yuan! Available online: https://www.163.com/dy/article/GB4L0939055004XG.html (accessed on 22 October 2021). (In Chinese)

15.	China Government Procurement Network. Huizhou 2021–2023 Catastrophe Insurance Service Procurement Project Winning Announcement. Available online: http://www.ccgp.gov.cn/cggg/dfgg/zbgg/202104/t20210430_16235384.htm (accessed on 22 October 2021). (In Chinese)

16.	China Government Procurement Network. Announcement of Catastrophe Insurance Service Procurement Project Results. Available online: http://www.ccgp.gov.cn/cggg/dfgg/zbgg/202108/t20210827_16787757.htm (accessed on 22 October 2021). (In Chinese)

17.	China Government Procurement Network. Announcement on the Winning Bid for the 2020–2023 Catastrophe Insurance Service Project (0835-200ZA9803341) of Maoming City Finance Bureau. Available online: http://www.ccgp.gov.cn/cggg/dfgg/zbgg/2 02101/t20210112_15787860.htm (accessed on 22 October 2021). (In Chinese)

18.	Dai, M. Guangzhou City Catastrophe Index Insurance Pilot Project Starts Typhoon and Heavy Rainfall to insure a total of 650 Million Yuan. Available online: http://news.ycwb.com/2019-03/20/content_30221804.htm (accessed on 22 October 2021). (In Chinese)

19.	China Government Procurement Network. Guangdong Province 2021–2023 Catastrophe Insurance Service Procurement Project Public Bidding Announcement. Available online: http://www.ccgp.gov.cn/cggg/dfgg/qtgg/202011/t20201125_15498762.htm (accessed on 22 October 2021). (In Chinese)

20.	China Government Procurement Network. Announcement on the Winning and Transaction of the 2020–2022 Catastrophe Index Insurance Project of Dongguan City Emergency Management Bureau. Available online: http://www.ccgp.gov.cn/cggg/dfgg/zb gg/202004/t20200410_14133309.htm (accessed on 22 October 2021). (In Chinese)

21.	Guangdong Zhongkai Engineering Management Consulting Co., Ltd. Dongguan Emergency Management Bureau Dongguan City 2020–2022 Catastrophe Index Insurance Project Public Bidding Announcement. Available online: http://ggzy.dg.gov.cn/ggz y/website/WebPagesManagement/TradeInfo/GovProcurement%20/govdetail?publishinfoid=3170510&fcInfotype=1 (accessed on 22 October 2021). (In Chinese)

22.	Jiangmen Public Resources Trading Network. 2019–2021 Jiangmen Catastrophe Index Insurance Project Winning Results Announcement. Available online: http://zyjy.jiangmen.cn/szqzcjggg/50743.htm (accessed on 22 October 2021). (In Chinese)

23.	China Government Procurement Network. Zhanjiang City Finance Bureau Zhanjiang City 2021–2023 Typhoon Catastrophe Insurance Project Won the Bid (Transaction) Announcement. Available online: http://www.ccgp.gov.cn/cggg/dfgg/zbgg/202 105/t20210525_16325709.htm (accessed on 22 October 2021). (In Chinese)

24.	Vickery, P.J.; Skerlj, P.F.; Twisdale, L.A. Simulation of Hurricane Risk in the US Using Empirical Track Model. *J. Struct. Eng.* **2000**, *126*, 1222–1237. [CrossRef]

25.	Emanuel, K.; Ravela, S.; Vivant, E.; Risi, C. A statistical Deterministic Approach to Hurricane Risk Assessment. *Bull. Am. Meteorol. Soc.* **2006**, *87*, 299–314. [CrossRef]

26.	Rumpf, J.; Weindl, H.; Höppe, P.; Rauch, E.; Schmidt, V. Stochastic Modelling of Tropical Cyclone Tracks. *Math. Methods Oper. Res.* **2007**, *66*, 475–490. [CrossRef]

27.	Rumpf, J.; Weindl, H.; Höppe, P.; Rauch, E.; Schmidt, V. Tropical Cyclone Hazard Assessment Using Model-Based Track Simulation. *Nat. Hazards* **2009**, *48*, 383–398. [CrossRef]

28.	Lee, C.-Y.; Tippett, M.K.; Sobel, A.H.; Camargo, S.J. An Environmentally Forced Tropical Cyclone Hazard Model. *J. Adv. Model. Earth Syst.* **2018**, *10*, 223–241. [CrossRef]

29.	Jing, R.; Lin, N. An Environment-Dependent Probabilistic Tropical Cyclone Model. *J. Adv. Model. Earth Syst.* **2020**, *12*, e2019MS001975. [CrossRef]

30.	RMS. RMS China Typhoon Model: Captures Risk from Wind, Inland Flood, and Storm Surge in China, Including Hong Kong and Macau. Available online: https://forms2.rms.com/rs/729-DJX-565/images/rms-china-typhoon-model-datasheet.pdf (accessed on 13 July 2021).

31. Ng, K.S.; Leckebusch, G.C. A New View on the Risk of Typhoon Occurrence in the Western North Pacific. *Nat. Hazards Earth Syst. Sci.* **2021**, *21*, 663–682. [CrossRef]

32. Osinski, R.; Lorenz, P.; Kruschke, T.; Voigt, M.; Ulbrich, U.; Leckebusch, G.C.; Faust, E.; Hofherr, T.; Majewski, D. An Approach to Build an Event Set of European Windstorms Based on ECMWF EPS. *Nat. Hazards Earth Syst. Sci.* **2016**, *16*, 255–268. [CrossRef]

33. Thompson, V.; Dunstone, N.J.; Scaife, A.A.; Smith, D.M.; Slingo, J.M.; Brown, S.; Belcher, S.E. High Risk of Unprecedented UK Rainfall in the Current Climate. *Nat. Commun.* **2017**, *8*, 107. [CrossRef] [PubMed]

34. Angus, M.; Leckebusch, G.C. On the Dependency of Atlantic Hurricane and European Windstorm Hazards. *Geophys. Res. Lett.* **2020**, *47*, e2020GL090446. [CrossRef]

35. Walz, M.A.; Leckebusch, G.C. Loss Potentials Based on an Ensemble Forecast: How Likely Are Winter Windstorm Losses Similar to 1990? *Atmos. Sci. Lett.* **2019**, *20*, e891. [CrossRef]

36. Leckebusch, G.C.; Renggli, D.; Ulbrich, U. Development and Application of an Objective Storm Severity Measure for the Northeast Atlantic Region. *Meteorol. Z.* **2008**, *17*, 575–587. [CrossRef]

37. Kruschke, T. Winter Wind Storms: Identification, Verification of Decadal Predictions, and Regionalization. Ph.D. Thesis, Freie Universität, Berlin, Germany, 2015. Available online: https://refubium.fu-berlin.de/handle/fub188/11913 (accessed on 22 October 2021).

38. Bougeault, P.; Toth, Z.; Bishop, C.; Brown, B.; Burridge, D.; Chen, D.H.; Ebert, B.; Fuentes, M.; Hamill, T.M.; Mylne, K.; et al. The THORPEX Interactive Grand Global Ensemble. *Bull. Am. Meteorol. Soc.* **2010**, *91*, 1059–1072. [CrossRef]

39. Swinbank, R.; Kyouda, M.; Buchanan, P.; Froude, L.; Hamill, T.M.; Hewson, T.D.; Keller, J.H.; Matsueda, M.; Methven, J.; Pappenberger, F.; et al. The TIGGE Project and Its Achievements. *Bull. Am. Meteorol. Soc.* **2015**, *97*, 49–67. [CrossRef]

40. Befort, D.J.; Kruschke, T.; Leckebusch, G.C. Objective Identification of Potentially Damaging Tropical Cyclones over the Western North Pacific. *Environ. Res. Commun.* **2020**, *2*, 031005. [CrossRef]

41. Hersbach, H.; Bell, B.; Berrisford, P.; Hirahara, S.; Horányi, A.; Muñoz-Sabater, J.; Nicolas, J.; Peubey, C.; Radu, R.; Schepers, D.; et al. The ERA5 Global Reanalysis. *Q. J. R. Meteorol. Soc.* **2020**, *146*, 1999–2049. [CrossRef]

42. Knapp, K.R.; Kruk, M.C.; Levinson, D.H.; Diamond, H.J.; Neumann, C.J. The International Best Track Archive for Climate Stewardship (IBTrACS) Unifying Tropical Cyclone Data. *Bull. Am. Meteorol. Soc.* **2010**, *91*, 363–376. [CrossRef]

43. Smith, A.; Lott, N.; Vose, R. The Integrated Surface Database: Recent Developments and Partnerships. *Bull. Am. Meteorol. Soc.* **2011**, *92*, 704–708. [CrossRef]

44. CMA. *Yearbooks of Meteorology in China*; China Meteorological Press: Beijing, China, 2000–2004. (In Chinese)

45. CMA. *Yearbooks of Meteorological Disaster in China*; China Meteorological Press: Beijing, China, 2005–2019. (In Chinese)

46. Chen, W.; Lu, Y.; Sun, S.; Duan, Y.; Leckebusch, G.C. Hazard Footprint-Based Normalization of Economic Losses from Tropical Cyclones in China during 1983–2015. *Int. J. Disaster Risk Sci.* **2018**, *9*, 195–206. [CrossRef]

47. Geiger, T.; Murakami, D.; Frieler, K.; Yamagata, Y. Spatially-Explicit Gross Cell Product (GCP) Time Series: Past Observations (1850–2000) Harmonized with Future Projections According to the Shared Socioeconomic Pathways (2010–2100). 2017. Potsdam Institute for Climate Impact Research by GFZ Data Services. Available online: https://dataservices.gfz-potsdam.de/pik/showshort.php?id=escidoc:2740907 (accessed on 22 October 2021). [CrossRef]

48. Geiger, T. Continuous National Gross Domestic Product (GDP) Time Series for 195 Countries: Past Observations (1850–2005) Harmonized with Future Projections According to the Shared Socio-Economic Pathways (2006–2100). *Earth Syst. Sci. Data* **2018**, *10*, 847–856. [CrossRef]

49. Lu, X.; Yu, H.; Lei, X. Statistics for Size and Radial Wind Profile of Tropical Cyclones in the Western North Pacific. *Acta Meteorol. Sin.* **2011**, *25*, 104–112. [CrossRef]

50. Shen, W.; Ginis, I.; Tuleya, R.E. A Numerical Investigation of Land Surface Water on Landfalling Hurricanes. *J. Atmos. Sci.* **2002**, *59*, 789–802. [CrossRef]

51. Choy, C.-W.; The Hong Kong Federation of Insurers; Wu, M.-C.; Lee, T.-C. Assessment of the Damages and Direct Economic Loss in Hong Kong Due to Super Typhoon Mangkhut in 2018. *Trop. Cyclone Res. Rev.* **2020**, *9*, 193–205. [CrossRef]

52. Ni, X.; Zhang, Q.; Ma, D.; Wu, L.; Ren, F. Climatology and Trends of Tropical Cyclone High Wind in Mainland China: 1959–2011. *J. Geophys. Res. Atmos.* **2015**, *120*, 12378–12393. [CrossRef]

53. Lee, T.-C.; Knutson, T.R.; Nakaegawa, T.; Ying, M.; Cha, E.J. Third Assessment on Impacts of Climate Change on Tropical Cyclones in the Typhoon Committee Region—Part I: Observed Changes, Detection and Attribution. *Trop. Cyclone Res. Rev.* **2020**, *9*, 1–22. [CrossRef]

54. Sibson, R. A Brief Description of Natural Neighbour Interpolation. In *Interpreting Multivariate Data*; Barnett, V., Ed.; Wiley: New York, NY, USA, 1981; pp. 21–36.

55. Geiger, T.; Frieler, K.; Levermann, A. High-Income Does Not Protect against Hurricane Losses. *Environ. Res. Lett.* **2016**, *11*, 084012. [CrossRef]

56. Mendelsohn, R.; Emanuel, K.; Chonabayashi, S.; Bakkensen, L. The Impact of Climate Change on Global Tropical Cyclone Damage. *Nat. Clim. Chang.* **2012**, *2*, 205–209. [CrossRef]

57. Klawa, M.; Ulbrich, U. A Model for the Estimation of Storm Losses and the Identification of Severe Winter Storms in Germany. *Nat. Hazards Earth Syst. Sci.* **2003**, *3*, 725–732. [CrossRef]

58. Gilleland, E.; Katz, R.W. extRemes 2.0: An Extreme Value Analysis Package in R. *J. Stat. Softw.* **2016**, *72*, 1–39. [CrossRef]

59. Gao, S.; Meng, Z.; Zhang, F.; Bosart, L.F. Observational Analysis of Heavy Rainfall Mechanisms Associated with Severe Tropical Storm Bilis (2006) after Its Landfall. *Mon. Weather Rev.* **2009**, *137*, 1881–1897. [CrossRef]

60. CMA. *Member Report: ESCAP/WMO Typhoon Committee 12th Integrated Workshop*; Jeju, Korea. 2017, p. 37. Available online: https://community.wmo.int/meetings/12th-session-escapwmo-typhoon-committee-integrated-workshop-iws-12 (accessed on 22 October 2021).

61. Yang, J.; Li, L.; Zhao, K.; Wang, P.; Wang, D.; Sou, I.M.; Yang, Z.; Hu, J.; Tang, X.; Mok, K.M.; et al. A Comparative Study of Typhoon Hato (2017) and Typhoon Mangkhut (2018)—Their Impacts on Coastal Inundation in Macau. *J. Geophys. Res. Ocean.* **2019**, *124*, 9590–9619. [CrossRef]

62. Mohleji, S.; Pielke, R. Reconciliation of Trends in Global and Regional Economic Losses from Weather Events: 1980–2008. *Nat. Hazards Rev.* **2014**, *15*, 04014009. [CrossRef]

63. Klotzbach, P.J.; Bowen, S.G.; Pielke, R.; Bell, M. Continental US. Hurricane Landfall Frequency and Associated Damage: Observations and Future Risks. *Bull. Am. Meteorol. Soc.* **2018**, *99*, 1359–1376. [CrossRef]

64. Pielke, R.A.; Gratz, J.; Landsea, C.W.; Collins, D.; Saunders Mark, A.; Musulin, R. Normalized Hurricane Damage in the United States: 1900–2005. *Nat. Hazards Rev.* **2008**, *9*, 29–42. [CrossRef]

65. McAneney, J.; Timms, M.; Browning, S.; Somerville, P.; Crompton, R. Normalised New Zealand Natural Disaster Insurance Losses: 1968–2019. *Environ. Hazards* **2021**, 1–19. [CrossRef]

66. Pielke, R. Economic 'Normalisation' of Disaster Losses 1998–2020: A Literature Review and Assessment. *Environ. Hazards* **2020**, *20*, 93–111. [CrossRef]

67. McAneney, J.; Sandercock, B.; Crompton, R.; Mortlock, T.; Musulin, R.; Pielke, R.; Gissing, A. Normalised Insurance Losses from Australian Natural Disasters: 1966–2017. *Environ. Hazards* **2019**, *18*, 414–433. [CrossRef]